Effect factors and evaluation method of part accuracy formed by ultrasonic micro punching with a flexible punch

Chang-tao Liu
Wei Liu
Xiao-guang Xu
Likuan Zhu (zhulikuan@yeah.net)
Shenzhen University https://orcid.org/0000-0002-0844-2677
Feng Luo

Research Article

Keywords: Micro punching, Ultrasonic, Thin copper sheet, Accuracy evaluation

Posted Date: February 7th, 2022

DOI: https://doi.org/10.21203/rs.3.rs-1311003/v1

Abstract

In this paper, an automatic and quick evaluating method for micro-hole size and form accuracy with computer-aided technique was proposed. Using this method, the form accuracy of the micro-hole punched by a special ultrasonic microforming method, that is Micro Ultrasonic thin Sheetmetal Forming using molten plastic as flexible punch (short as Micro-USF), was discussed. Using this microforming method, micro-holes with diameters of 500,600 and 700 mm were punched from a thin sheet of purple copper with a thickness of 30 mm. The experimental results showed that the ratios of the maximum size error and the maximum roundness error of the micro-hole to the corresponding punching die diameter were 1.40% and 1.47%, respectively, and the ratios of the maximum size error range and the maximum form error range to the corresponding punching die diameter were 0.70% and 0.72%, respectively, indicating that this Micro-USF method has high accuracy and precision for punching micro-holes. Moreover, it was found that there is no significant direct correlation between micro-holes sample errors and these forming parameters when the forming parameters such as ultrasonic power, ultrasonic time and cylinder pressure were varied, which indicated that the sample errors were random in some extent.

1 Introduction

With the development of micro-electro-mechanical systems (MEMS), the demand of micro-holes parts in manufacturing industry is increasing. The processing quality (such as size and form accuracy) of micro-holes largely determines the quality of the MEMS product [1, 2]. At present, the methods of processing micro-hole mainly include micro-drilling, electro-chemical drilling ,micro-electro-discharge forming and micro punching[3]. Among them, the micro punching is becoming more and more important and popular due to its advantages such as simple process, high quality and high processing efficiency [4, 5].

In order to improve the punching quality, it is important to find a proper way to characterize and evaluate the micro-hole shape. Optical microscopy techniques, atomic force microscopy (AFM), scanning electron microscope (SEM), focused ion beam imaging microscope (FIBM) are currently common methods to determine the size and form of micro-holes [6]. Although AFM, SEM and FIBM are able to achieve high accuracy of morphological characterization by atomic-level contact with the part's surface, the measurement time increases dramatically as the measurement size increases [7–9]. In contrast, for sub-millimeter micro-holes, the microscope technique is a faster and more accurate method to obtain the micro-hole contour and evaluate its size and form accuracy, which is widely used in micro scale characterizing process[10, 11].

However, based on a specific morphological characterization method, there is no unified standard on how to properly evaluate the accuracy of micro-hole forming. Considering the deviations in size and form are easy to happen for micro-holes obtained by most of punching methods, the evaluation of the form accuracy becomes an important basis for determining whether the micro-hole meets the requirements of the application. These literatures [12, 13] directly calculated the difference between the micro-hole diameter and the die hole diameter as the size deviation of the micro-holes. The literature[14] used the

difference between the maximum and minimum radius of the micro-hole contour as its roundness error. The literature[15]measured the micro-hole diameter in four directions (0∘,45∘,90∘,135∘) and used the maximum difference among the data (*Dmax−Dmin*) to represent the roundness error. The literature[16]evaluated the accuracy of punched hole by calculating the difference between the punched hole diameter and die hole diameter. In the literature[17], the outer contour of the hole was first measured for a small hole with a diameter of about 1 mm using a universal projector. Then the outer contour of the hole was divided into 36 equal parts at 10° intervals, and subsequently the polar coordinate form was established with the center of the contour circle as the coordinate origin. Finally, the least squares circle radius of the micro-hole was determined according to the 36 equal parts circle radius, and the accuracy of small hole forming could be evaluated consequently.

In order to evaluate the accuracy of micro-hole formed by punching quickly and accurately, this paper proposed a rapid determination and evaluation method of micro-hole diameter size and roundness error by combining micro-imaging technology and computer-aided image processing technology. This method was then used to analyze the size and form accuracy of micro-holes punched by Micro-USF[18], and the effects of ultrasonic power, ultrasonic time and cylinder pressure on the forming quality of micro punching holes were also investigated.

2 Micro-hole Size Measurement And Roundness Error Evaluation

This paper first extracted the contour of the micro-hole, and then used the extracted contour to measure and evaluate the size of micro-hole and roundness error respectively.

2.1 Micro-hole image processing and contour extraction

The basic process of micro-hole contour extraction was shown as following:

(1) Color photo decolorization and pixel region analysis

Figure 1a showed a micro-hole photo from a microscope which was first decolorized and converted to a grayscale image for the micro-hole contour extraction step (Fig. 1b). A certain part of the micro-hole contour (Fig. 1b) was enlarged (Fig. 1c). As seen in Fig. 1c, the micro-hole contour and its nearby region were composed of pixels. From Fig. 1c, a virtual boundary could be distinguished between the upper right corner and the lower left corner, which divided the whole photo into two triangular regions (lower left and upper right). The lower left darker region was the inner part of the hole. The brighter region on the upper right was the surface part of the hole. The transition region between these two parts was the micro-hole contour region. Fig. 1d was an enlargement of the local region in Fig. 1c, where the small red rectangle meant a pixel, and the grayscale value of each pixel was added later. The grayscale of the pixel took the value interval from 0 to255,0 for pure black and 255 for pure white, and the different grayscale values represented their different shades of gray.

(2) Grayscale value normalization

When taking photos of micro-holes with a microscope, the overall brightness of the photos taken at different times was often different because the light brightness might vary. In order to extract the micro-holes contours from various photos accurately with a uniform method, it was necessary to firstly normalize the grayscale values in the grayscale image. The method of processing was shown in Fig. 2. Region A was the inner part of the micro-hole, B represented the region where the contour of the micro-hole is located, and C meant the surface region of the micro-hole (Fig. 2).

The average grayscale values in the hole region A and the hole surface region C were firstly calculated. For example, the measured average grayscale value of all pixels in region A in Fig. 2a was 41, and the average grayscale value of all pixels in region C was 170. Considering the region inside the hole should be black, the region on the surface of the hole should actually be white. Therefore, all grayscale values below the average value of 41 in region A were set to 0, all grayscale values above the average value of 170 in region C were set to 255, and other pixels with grayscale values from 41 to 170 were mapped to the interval from 0 to 255. This mapping relationship was shown in Fig. 2b. The transformed image was shown in Fig. 2c.

Figure 3 was consist of color photos and images processed in Sections (1) and (2) above. The first column "Original photos" was the original photos with three different light brightness (Figure 3). The second column showed the images after the above Section (1) for color decolorization, and the third column "After normalization" was for the images obtained after the normalization process in Section (2) above. After such processing, the effect of different image brightness was eliminated, and the foundation was laid for the extraction of micro-hole contour by thresholding later.

(3) Threshold determination and image binarization

The threshold value was calculated using the Otsu method which used the interclass variance expression to obtain 256 interclass variance values between the region A (foreground black) and the region C (background white) of the hole surface by traversing all grayscale values in the interval from 0 to 255. The larger the interclass variance value between foreground black and background white, the greater the difference between foreground and background, which indicated that the grayscale value with the largest interclass variance was the desired threshold value. After obtaining the threshold value, all grayscale values below the threshold were set to 0 and grayscale values above the threshold were set to 255, which transformed the previously processed image to a binary image. Processing images with the Otsu method was simple and efficient, which could be considered as an adaptive method for determining threshold.

(4) Micro-hole contour extraction

After the above binarization process, the black and white border edge in the binary image could be identified as the micro-hole contour. The above image processing was programmed using MATLAB software. The original photos of the micro-hole were input for processing, and the micro-hole contours extracted from the photos with different light brightness were shown in Fig. 4. The image was replaced with the original color photos, which was for extracting the micro-hole contours more accurately (Fig. 4).

As seen in Fig. 4, the extracted micro-hole contours were basically consistent with the usual observations, while the extracted micro-hole contours were the same even if the brightness values of the original photos taken were different. Thus, it could be seen that the micro-hole contour could be determined more easily and more accurately using the prepared procedure.

2.2 Determination of micro-hole diameter and roundness error evaluation

As shown in Fig. 5, the least-squares circle was used as the ideal element to evaluate the actual circle of the micro-hole contour when the contour of the micro-hole was extracted. The diameter of the least-squares circle was used to represent the actual diameter *Da* of the micro-hole. Meanwhile, the maximum external circle and the minimum internal tangent circle of the contour concentric with the least squares circle were determined, and the radius difference *r* between the two circles was calculated to represent the roundness error of the micro-hole.

By incorporating all of the above image processing and error evaluation into a program prepared by MATLAB software, the micro-hole size and roundness error could be measured and evaluated easily and quickly. It should be mentioned that the whole process took only about 20s to evaluate a micro-hole.

3 Experiment

3.1 Forming principle of Micro-USF

Figure 6 showed the principle of the Micro-USF used to the micro punching process. Before starting the punching experiment, fix the baseplate, place the die on the baseplate, place the thin sheetmetal in the middle of the die and the pressure plate, then fix the pressure plate on the baseplate with screws, and finally put the plastic powder into the stock bin.

In the punching experiment, the ultrasonic vibration starts to be applied when the ultrasonic punch is lowered into contact with the plastic powder in the stock bin and compressed. Under the effect of ultrasonic vibration, the plastic powder in the stock bin will rub and collide with each other, which could cause the plastic powder to be melt into a viscous fluid medium to form a flexible punch. The flexible punch could transmit ultrasonic punch pressure and ultrasonic vibration to the sheetmetal to create a micro-punched sample after shear fracture along the perimeter of the die hole.

In this microforming method, the ultrasound vibration could melt the plastic powder to form a flexible punch and was also transmitted to the thin sheetmetal through the molten plastic. Therefore, this method belonged to an ultrasound-assisted microforming method, and its advantages [19, 20] could be effectively utilized.

3.2 Experimental platform

The Micro-USF experimental platform was consist of an ultrasonic plastic welding machine and a set of special micro punching experimental set-up. The main pressure of the ultrasonic punch was provided by the air cylinder built into the ultrasonic plastic welding machine, and the ultrasonic welding machine also generated ultrasonic vibration on the ultrasonic punch. The 2020 ultrasonic plastic welding machine

produced by Shenzhen RIFA Ultrasonic Equipment Co., Ltd. was used in the experiment, and its main parameters were shown in Table 1. The special micro-punching experimental set-up was shown in Fig. 6, which was mainly composed of a baseplate, a pressure plate, stock bin and some screws.

Table 1
Main parameters of RIFA 2020 ultrasonic plastic welding machine

Max power	output frequency	Cylinder pressure	Ultrasonic power	Ultrasonic time
2080 W	20 kHz	0 ~ 0.6 MPa	50 ~ 100%	0 ~ 9.99 s

3.3 Die

The material of the die is Cr12MoV(Chinese national standard GB/T 1299-1985) die steel plate with 1mm thickness, and round through holes were machined by mechanical method. The actual dies were shown in Fig. 7.

In this paper, three dies with different micro-hole diameters were used, and their design diameters were 500, 600, 700 mm respectively. Their actual diameters and roundness errors were measured by the methods described in Section 2, and the results were shown in Table 2.

Table 2
Die design diameters, actual diameters and roundness errors (unit: mm)

Design diameters *d*	Actual diameters *dd*	Roundness errors *rd*
500	502.72	9.50
600	607.32	9.68
700	713.80	11.64

3.4 Experimental materials

The experimental material was T2 purple copper (Chinese national standard GB/T 5231-2012) and its chemical composition and material properties were shown in Table 3 and Table 4, respectively. The thickness of T2 thin copper sheet with rolled state used in the experiments was 30 μm.

Table 3
Chemical composition of T2 purple copper (%)

Cu+Ag	Bi	Sb	As	Fe	Pb	S
≥99.90	≤0.001	≤0.002	≤0.002	≤0.005	≤0.005	≤0.005

Table 4
Material properties of T2 purple copper

Elastic modulus (GPa)	Yield strength (MPa)	Tensile strength (MPa)	Elongation (%)	Brinell hardness (HBS)
120	300-380	400-500	4-6	110-130

The material for the flexible punch was EVA (Ethylene Vinyl Acetate) plastic powder with an average particle size of 350 mm, and its melting temperature was 90°C.

3.5 Experiment process

The samples obtained from the experiments could be divided into 3 categories, as shown in Fig. 8. In the first category in which the experimental parameters were small, the punching could not be completed, as in the samples shown in Fig. 8a and Fig. 8b. In the second category in which the experimental parameters were large, the samples fractured, as in the sample shown in Fig. 8c. The samples in the two categories of Figs. 8abc were not fully formed. In the third category in which the punched sample was a completely round hole and no fracture happened, and this sample was considered to be fully formed, as shown in Fig. 8d.

For the Micro-USF method, ultrasonic power, ultrasonic time and cylinder pressure were three important parameters of affected micro punching. In the experiment, the other parameters were kept constant and the above three parameters were changed to study their effects on the form accuracy of micro-hole sample punched by Micro-USF. In each set of parameters, 8 samples were punched out, and if 5 or more were fully formed, 5 were selected for measurement and data were recorded. If only 4 or less samples were fully formed, the samples were considered as not fully formed at that parameter and were discarded from the discussion. In this paper, the parameters for obtaining fully formed samples were: ultrasonic power 50%-70%, ultrasonic time 0.4 s-0.6 s and cylinder pressure 0.1 MPa-0.5 MPa,

3.6 Micro-hole accuracy evaluation

Considering that there was an error between the actual diameter size and design size of the die, and the roundness error of the die might be transferred to the sample, the effect of die error should be deducted in the sample error evaluation. Therefore, the difference *fd* between the sample size and the actual diameter size of the die was used to evaluate the size accuracy of the punched sample, and the difference *fr* between the sample roundness error and the die roundness error was used to evaluate the form accuracy of the punched sample. That was:

$$f_d = d_d - d_s \quad (1)$$

Here, *fd* is the size error of the sample relative to the die, *dd* is the measured diameter of the die, and *ds* is the measured diameter of the sample.

$$f_r = r_s - r_d$$

2

Here, *fr* is the roundness error of the sample relative to the die, *rd* is the die roundness error, and *rs* is the sample roundness error.

4 Results And Discussion

The experimental results obtained by punching with the aforementioned three different diameter of dies were as follows.

For the effect of ultrasonic power on sample error, the ultrasonic power was taken as 55%, 60%, 65% and 70% at ultrasonic time of 0.4 s and cylinder pressure of 0.1 MPa respectively, and the average values of the obtained sample size error *fd* and roundness error *fr* and their ranges were shown in Fig. 9.

For effect of ultrasonic time on sample error, the ultrasonic time was taken as 0.45 s, 0.50 s, 0.55 s and 0.60 s at the ultrasonic power of 50% and the cylinder pressure of 0.1 MPa respectively, and the average values of the obtained sample size error *fd* and roundness error *fr* and their ranges were shown in Fig. 10.

For effect of cylinder pressure on sample error, the cylinder pressure was taken as 0.2 MPa, 0.3 MPa, 0.4 MPa and 0.5 MPa at ultrasonic power of 50% and ultrasonic time of 0.4 s respectively, and the average values of the obtained sample size error *fd* and roundness error *fr* and their ranges were shown in Fig. 11.

The lower limit of the error bars of the roundness error was found negative for the 700 mm samples at the ultrasonic powers of 55% and 65% in Fig. 9b and at the ultrasonic time of 0.55 s and 0.60 s in Fig. 10b, which indicated that the roundness error of some samples was smaller than that of the die (Equation (2)). This was mainly due to that the die with 700 mm diameter had a larger roundness error (see Table 2). That is, some larger form accuracy deviations between the actual edge to the ideal circumference of the die hole were not fully reflected on the punching sample, which caused the roundness error of the sample was less than that of the die.

From the experimental results shown from Fig. 9 to Fig. 11, the maximum values of size error *fd* and roundness error *fr* were 8.48 mm and 8.45 mm, respectively, and the maximum values of the ratio of size error and roundness error to the actual diameter of its corresponding die were 1.40% and 1.47%, respectively, indicating that the Micro-USF method had a high degree of form accuracy. On the other hand, the maximum values of the range of size error *fd* and roundness error *fr* (i.e., the length of the error bars in Fig. 9-Fig. 11) were 4.09 mm and 4.19 mm, respectively, and the maximum values of the ratio of the range of size error and roundness error to the actual diameter of the die were 0.70% and 0.72%, respectively, indicating that the micro-hole punched by the Micro-USF method had a high form precision.

In Fig. 9-Fig. 11, the bar height in the bar graph represented the average deviation of the sample size or roundness error from the actual size and roundness error of the die hole under a certain experimental condition. Although the sample error also changed as the experimental condition varied, as shown in the change of ultrasonic power from 55–70% (Fig. 9a). But on the other hand, the amount of this change was relative small to the corresponding error range (the length of the error bars in the Fig. 9), and there was a

certain overlap between the error value intervals reflected by the error bars for each experimental condition (e.g., 55%, 60%, 65%, and 70% of ultrasonic power in Fig. 9a). Within the error range reflected by the error bar, it was possible to obtain samples with errors in this range. Therefore, the average error values (height of the bars in the bar graph) of the five selected samples changed with the choice of samples, which leaded to an essential change in the variation curve. For example, for the 500 mm samples in Fig. 9a, as the ultrasonic power changed from 55–60%, it was possible that the curve might change from decreasing to increasing if the selected sample was different. This was because the lower end of the 500 mm sample error bar at 55% ultrasonic power was lower than the average value of the sample error at 60% ultrasonic power. This indicated that changing the forming parameters did not directly affect the change in the sample error. That is to say that there was a randomness in the sample error that was not significantly and directly related to the forming parameters.

Dividing the range of all errors (error bar lengths) in Fig. 9-Fig. 11 by the corresponding actual diameters of the die micro-holes, the values lie in the interval from 0–0.72%. Within such a small interval, a certain slight effect could lead to a change in the results, so the effect of random factors dominated the errors obviously. This probably was the reason why the sample errors show randomness.

5 Conclusion

The main research work and conclusions of this paper were as follows.

(1)A method for rapid evaluation of micro-hole size and roundness errors was proposed. Based on the microscope imaging, the actual contour of the micro-hole was obtained by image processing, and the micro-hole size and roundness error was evaluated by the least square method.

(2) Using the Micro-USF technique to punch micro-holes with different diameters in thin T2 copper sheets with thickness of 30 mm, the experimental results showed that the technique has a high degree of form accuracy and form precision. However, the sample error and the forming parameters such as ultrasonic power, ultrasonic time and cylinder pressure, do not show a direct correlation, which indicates that the sample error is random in some extent.

Declarations

Author contributions Chang-tao Liu wrote the programs, conducted the experiments and wrote the original draft. Wei Liu conducted a part of the experiments. Xiao-guang Xu tested the samples. Li-kuan Zhu analyzed the data, reviewed and modified the manuscript. Feng Luo made the overall plan, drew the pictures, and provided a fund support.

Funding This work is supported by the National Natural Science Foundation of China (Grant Nos. 51775351).

Conflict of interest The authors declare no competing interests.

References

1. Xu J, Guo B, Shan D, Wang C, Wang Z (2013) Surface quality improvements of WC–Co micro-punch finished by ion beam irradiation for micro-punching process of metal foil. Surf Coat Tech 235:803–810
2. Hyacinth Suganthi X, Natarajan U, Ramasubbu N (2015) A review of accuracy enhancement in microdrilling operations. Int J Adv Manuf Technol 81(1):199–217
3. Xu J, Guo B, Shan D, Wang Z, Li M, Fei X (2014) Micro-punching process of stainless steel foil with micro-die fabricated by micro-EDM. Microsyst Technol 20(1):83–89
4. Geiger M, Kleiner M, Eckstein R, Tiesler N, Engel U (2001) Microforming CIRP Ann 50(2):445–462
5. Vollertsen F, Schulze Niehoff H, Hu Z (2006) State of the art in micro forming. Int J Mach Tool Manu 46(11):1172–1179
6. Yang Y, Dong Z, Meng Y, Shao C (2021) Data-Driven Intelligent 3D Surface Measurement in Smart Manufacturing: Review and Outlook. Machines 9(1):13–45
7. Garcia R, Knoll AW, Riedo E (2014) Advanced scanning probe lithography. Nat Nanotechnol 9(8):577–587
8. Soleimani M, van Breemen LCA, Maddala SP, Joosten RRM, Wu H, Schreur-Piet I, van Benthem RATM, Friedrich H (2021) In Situ Manipulation and Micromechanical Characterization of Diatom Frustule Constituents Using Focused Ion Beam Scanning Electron Microscopy. Small Methods 5(12):2100638–2100647
9. Hashimoto Y, Shigeto K, Komatsuzaki R, Saito T, Sekiguchi T (2021) Damage-less observation of polymers by electron dose control in scanning electron microscope. J Electron Microsc 70(4):375–381
10. Middya S, Curto VF, Fernandez-Villegas A, Robbins M, Gurke J, Moonen EJM, Kaminski Schierle GS, Malliaras GG (2021) Microelectrode Arrays for Simultaneous Electrophysiology and Advanced Optical Microscopy. Adv Sci 8(13):2004434–2004442
11. Sheppard CJR (2021) The Development of Microscopy for Super-Resolution: Confocal Microscopy, and Image Scanning Microscopy. Appl Sci 11(19):8981–9000
12. Yu Z, Li D, Yang J, Zeng Z, Yang X, Li J (2019) Fabrication of micro punching mold for micro complex shape part by micro EDM. Int J Adv Manuf Technol 100(1–4):743–749
13. Xu J, Guo B, Shan D, Wang C, Li J, Liu Y, Qu D (2012) Development of a microforming system for micro-punching process of micro-hole arrays in brass foil. J Mater Process Technol 212(11):2238–2246
14. Joo B-Y, Rhim S-H, Oh S-I (2005) Micro-hole fabrication by mechanical punching process. J Mater Process Technol 170(3):593–601
15. Chern G-L, Wu Y-JE, Liu S-F (2006) Development of a micro-punching machine and study on the effect of vibration machining in micro-EDM. J Mater Process Technol 180(1):102–109
16. Rhim SH, Son YK, Oh SI (2005) Punching of Ultra Small Size Hole Array. CIRP Ann 54(1):261–264

17. Endo H, Murahashi T, Marui E (2007) Accuracy estimation of drilled holes with small diameter and effect of drill parameter on the machining accuracy when drilling in mild steel sheet. Int J Mach Tool Manu 47(1):175–181
18. Xiao Y, Sun F, Ran J-q, Wang B, Zhong J-m, Ma J, Luo F (2020) Ultrasonic micro punching with flexible punch for thin stainless sheet metal. Int J Adv Manuf Technol 108(9):2763–2773
19. Liu Y, Wang C, Han H, Shan D, Guo B (2017) Investigation on effect of ultrasonic vibration on micro-blanking process of copper foil. Int J Adv Manuf Technol 93(5):2243–2249
20. Wang C, Liu Y, Wan S, Guo B, Shan D, Zhang B (2019) Effect of Ultrasonic Vibration on Deformation in Micro-blanking Process with Copper Foil. J Wuhan Univ Technol 34(2):404–409

Figures

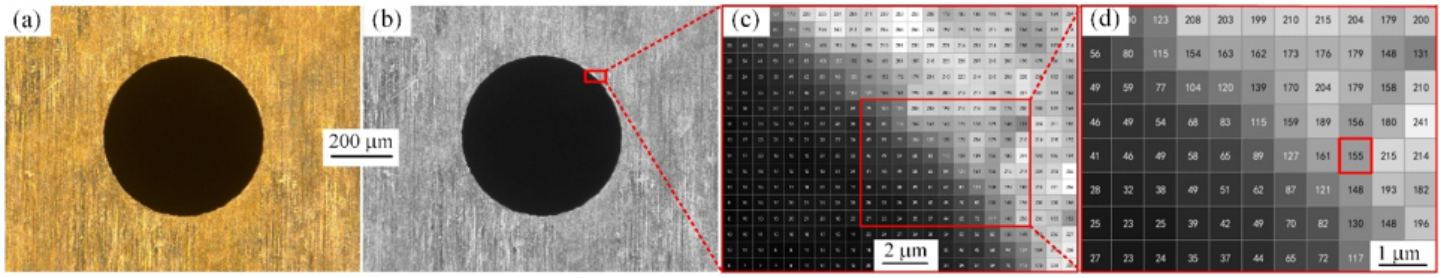

Figure 1

Color photo decolorization and grayscale value levels of pixels. (a) Color photo taken by microscope (b) Grayscale image obtained after color photo decolorization (c) Enlarged view of the micro-hole contour and its nearby region (d) Pixels and their grayscale values

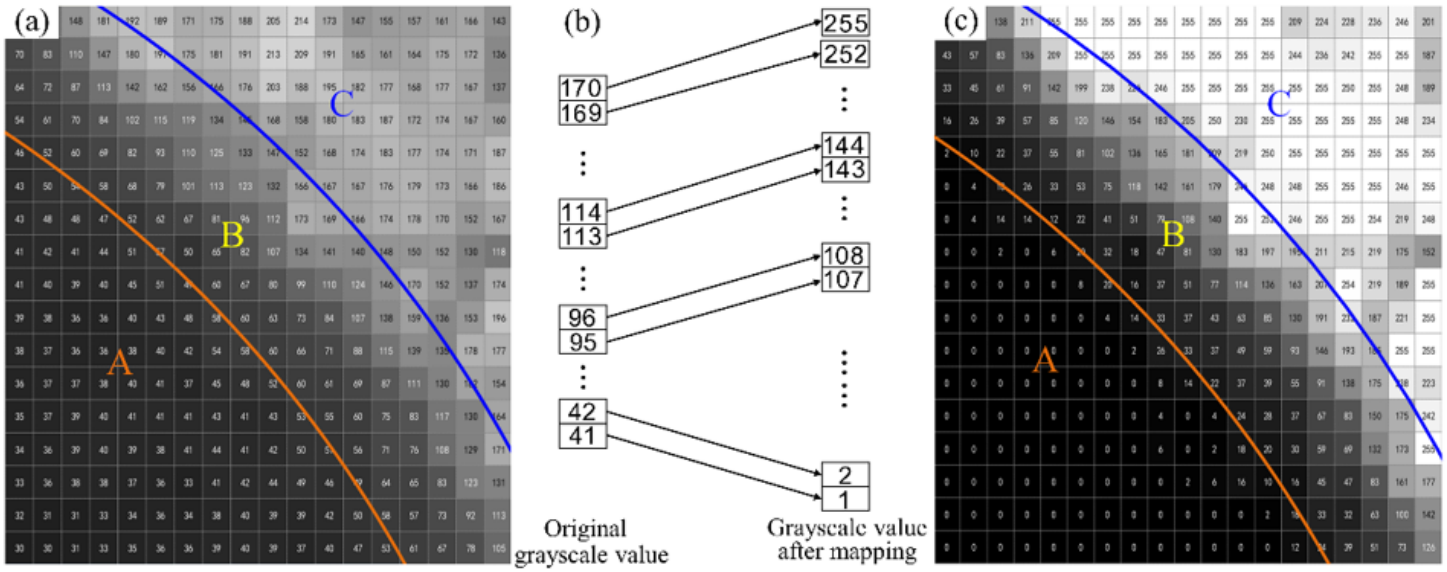

Figure 2

Grayscale value normalization. (a) Enlarged view of the micro-hole contour and nearby region on the image before processing. (b) Mapping relationship of grayscale values (c) Enlarged view of the micro-hole contour and nearby region on the image after processing.

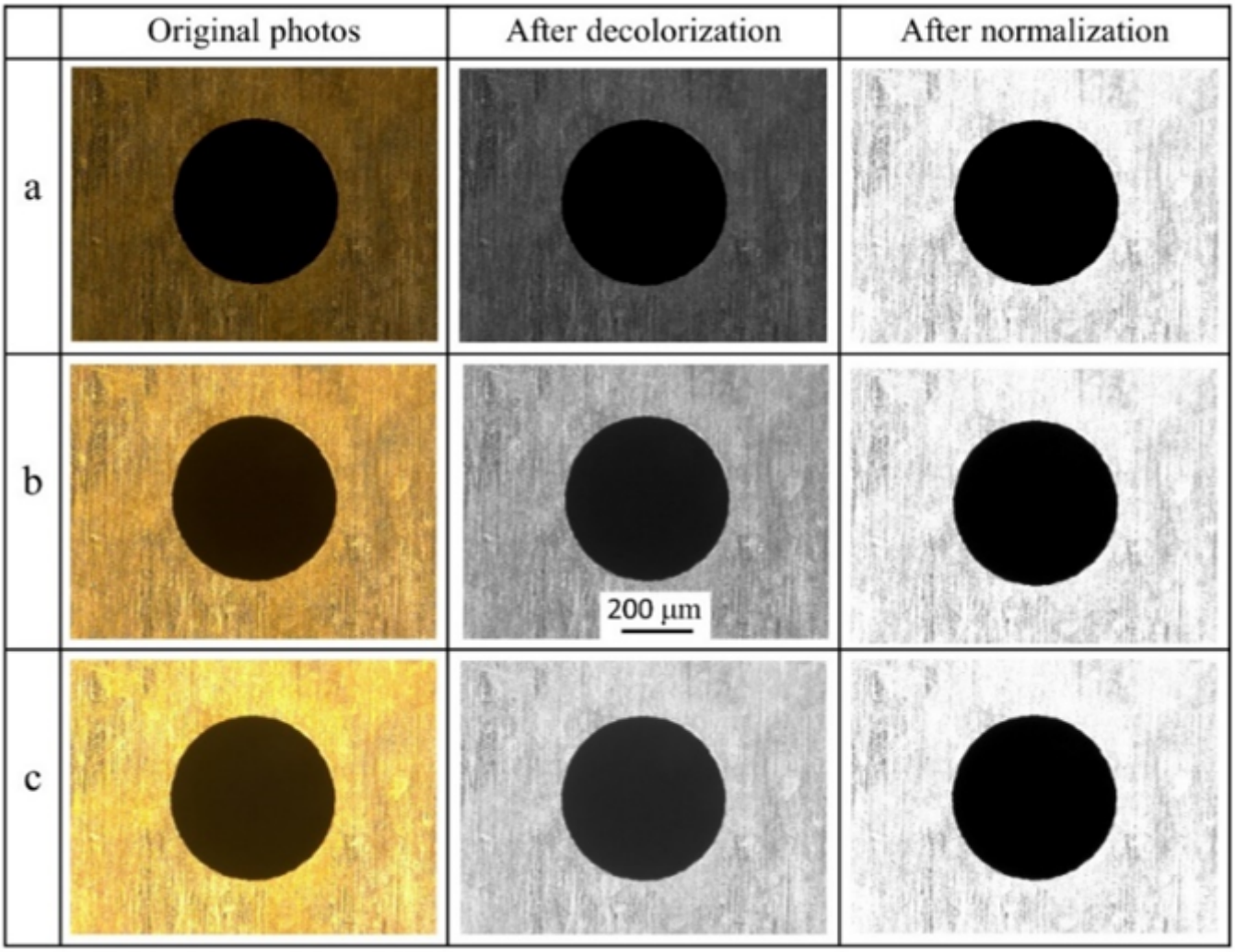

Figure 3

Comparison of micro-holes photos before and after normalization treatment under different light brightness. (a) Photo taken at 20% light brightness (b) Photo taken at 40% light brightness (c) Photo taken at 60% light brightness

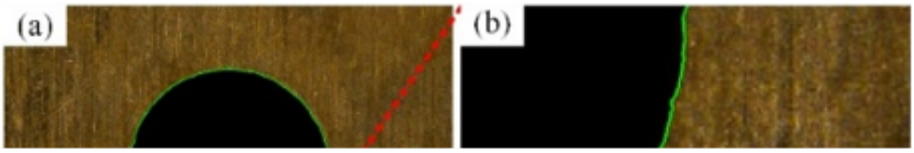

Figure 4

The extracted micro-hole contours for the same sample with different brightness values at the same location. (a)(c)(e) Photos taken at 20%, 40%, and 60% light brightness, respectively. (b)(d)(f) Enlarged views of the micro-hole contour and its nearby region corresponding to photos (a)(c)(e), respectively.

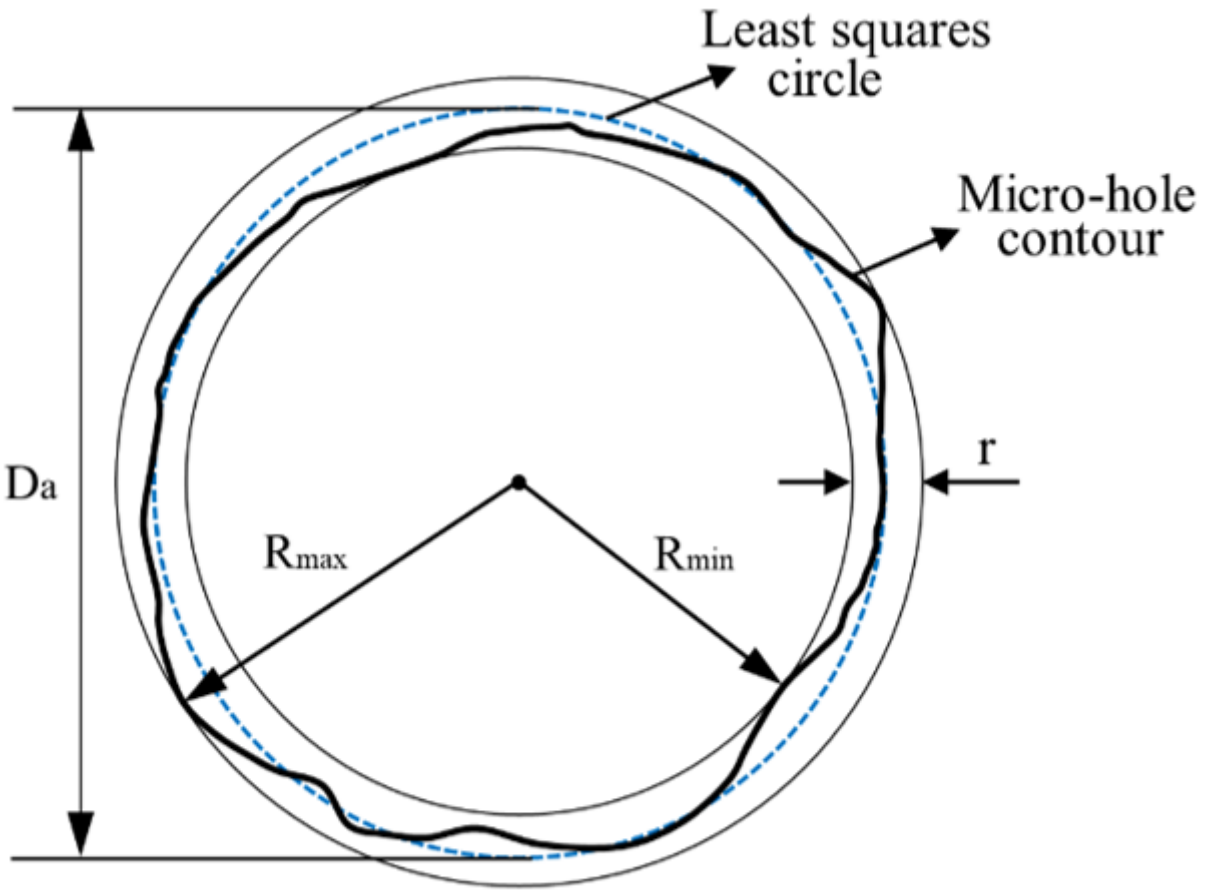

Figure 5

Evaluation of micro-hole contour and roundness error

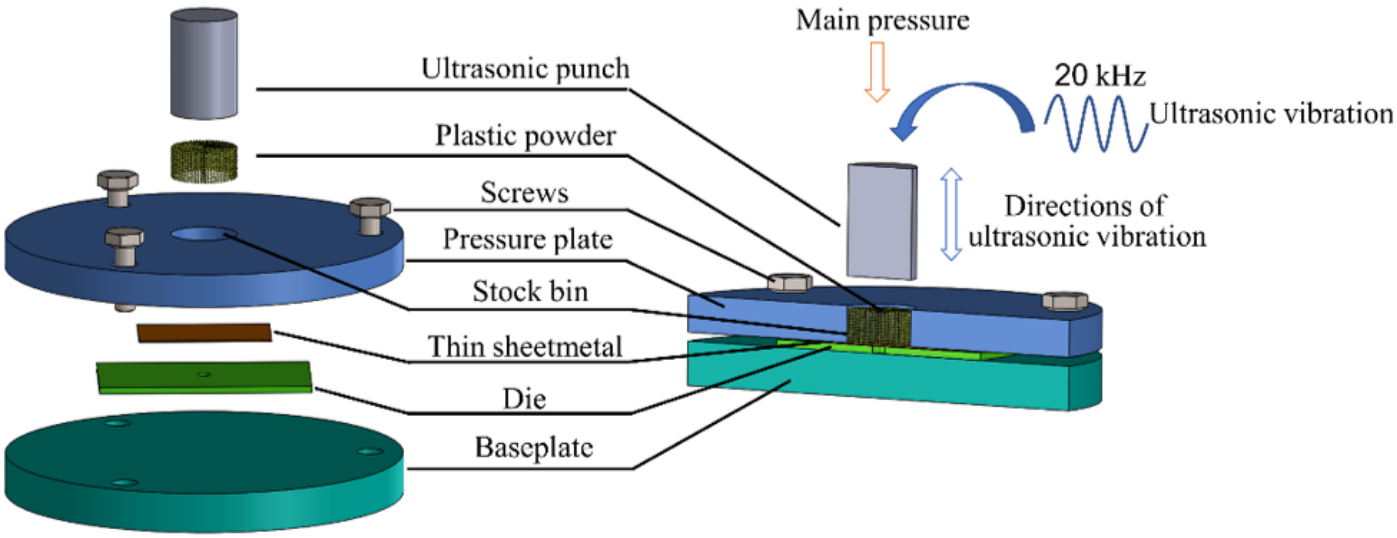

Figure 6

Principle of the Micro-USF used to the micro punching process

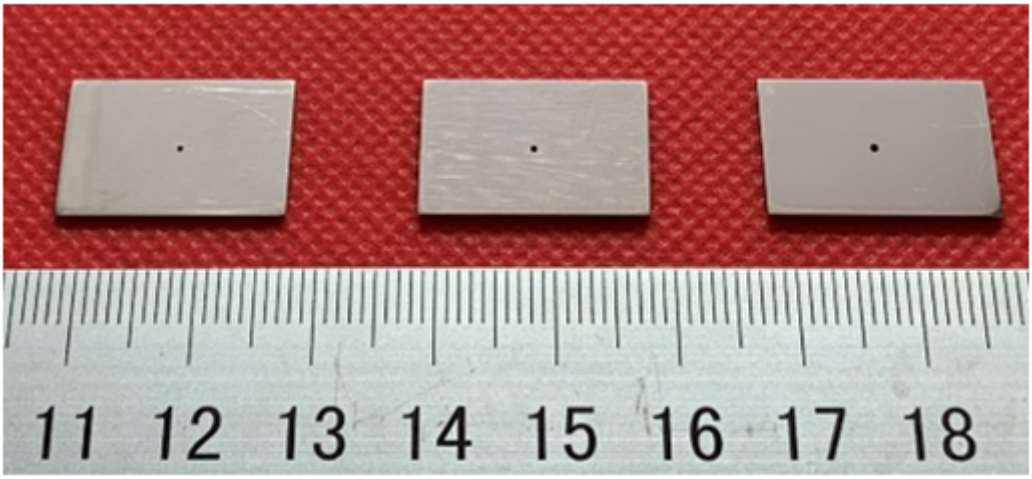

Figure 7

Photo of the three dies with different diameters

Figure 8

Various categories of samples appearing during micro punching experiments

(a) Sample not punched through (b) Sample not fully formed (c) Sample fracture (d) Fully formed sample

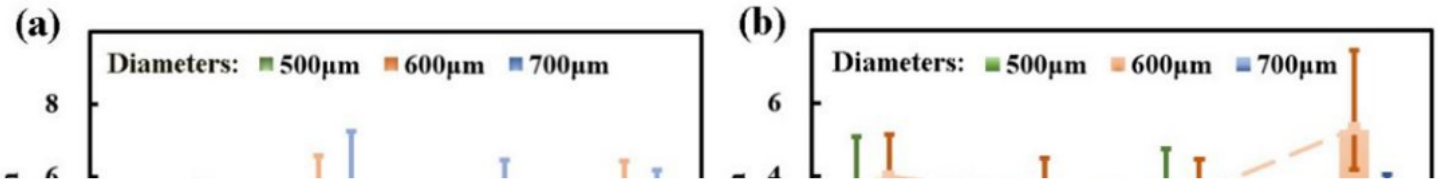

Figure 9

Effect of varying the ultrasonic power on the sample error when the values of ultrasonic time and cylinder pressure were 0.4 s and 0.1 MPa, respectively. (a) Size error *fd* (b) Roundness error *fr*

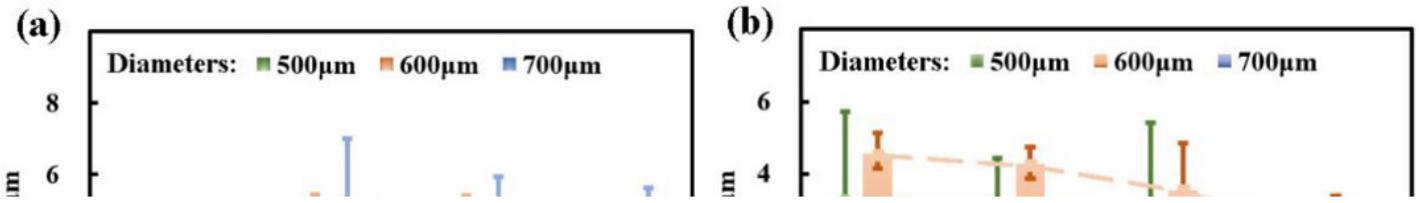

Figure 10

Effect of varying the ultrasonic time on the sample error when the values of ultrasonic power and cylinder pressure are 50% and 0.1 MPa, respectively. (a) Size error *fd* (b) Roundness error *fr*

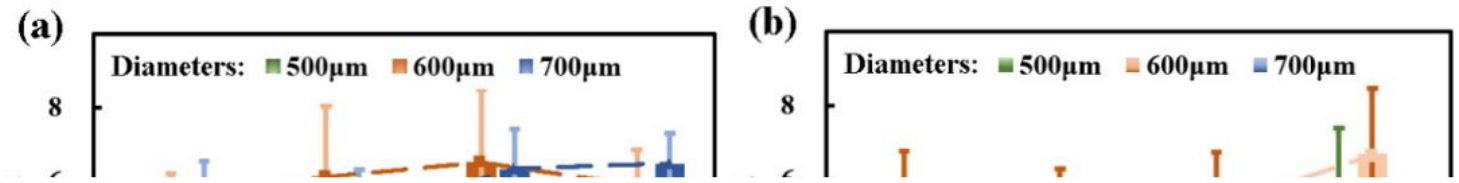

Figure 11

Effect of varying the cylinder pressure on the sample error when the values of ultrasonic power and ultrasonic time were 50% and 0.4 s, respectively.(a) Size error *fd* (b) Roundness error *fr*.